CrystEngComm

Accepted Manuscript

ROYAL SOCIETY OF CHEMISTRY

www.rsc.org/crystengcomm

Journal Name

COMMUNICATION

Experimental and Theoretical Investigation of a Stable Zinc-Based Metal-Organic Framework for CO_2 Removal from Syngas†

Received 00th January 20xx,
Accepted 00th January 20xx

DOI: 10.1039/x0xx00000x

www.rsc.org/

Ruiqin Zhong,[*,a] Jia Liu,[b] Xing Huang,[a] Xiaofeng Yu,[a] Changyu Sun,[a] Guangjin Chen,[a] and Ruqiang Zou[*,b]

A stable Zn-based metal-organic framework has been synthesized and applied for CO_2 removal from syngas composed of CO and H_2 for the first time. Further study in combination with Monte Carlo and ideal adsorbed solution theory method demonstrates the CO_2 adsorption behavior and separation performance which has been further confirmed by breakthrough experiment.

In recent years, CO_2 capture technologies become more and more significant and continually developed to reduce the amount of greenhouse gas that contributes to global climate change. Besides the electricity generation and the combustion of fossil fuels in transportation, industry is one of the main sources of CO_2 emission, as reported by the U.S. Environmental Protection Agency.[1] Syngas, a fuel gas mixture consisting primarily of H_2 and CO, is one of the most important reagents utilized in refineries, chemical processes and power generation.[2] The removal of CO_2 from syngas is not only essential in the fight against climate change,[3] but also greatly beneficial to the promotion of energy efficiency and conservation in many chemical reactions.

Metal-organic frameworks (MOFs) as a relative new family of crystalline and porous materials, are constructed by metal-ligand coordination bond and/or intermolecular weak interactions.[4] Thanks to their intriguing properties, such as ultra-high surface area, well-ordered pore structures and modifiable chemical functionality, MOFs have shown improved performance for adsorption-based CO_2 separation[5], especially for binary mixtures of CO_2/H_2,[6] or CH_4/CO_2,[7] CH_4/H_2,[8] in comparison to many conventional industrial adsorbents like zeolites, active carbons.[9] Mg_2(dobdc), known as MOF-74, exhibits the highest CO_2 uptake of 5.3 mmol/g (18.9 wt %) at 0.15 bar and 313 K compared with any solid adsorbent under these conditions.[10] The high potential application of MOF for syngas purification has been proposed by Jiang group that reported a charged *soc*-MOF for syngas purification could reach a selectivity of 600 at 298 K and 300 kPa using atomistic simulations.[11] It should be noted that the syngas was designated as H_2, and the syngas purification only referred to the separation of H_2 from CO_2/H_2 mixture.

However, the real application of MOFs in industry also lies on their structural stability in the presence of water vapour or moist air which is almost unavoidable and cannot be neglected in industrial environment.[12] For example, IRMOFs,[13] one of the archetypical families of MOFs featured by oxide-centered Zn_4O tetrahedral clusters and widely studied as candidates for gas separation and catalysis, will experience the framework's collapse at very low water contents of 6wt% at room temperature.[14] It is also a great pity for Mg-MOF-74 that a significant decrease in CO_2 adsorption was observed after the exposure to water.[15] Therefore, more efforts for a better understanding of the critical contributors to the water sensitivity and more investigations on new generation of MOFs with both target function and proper water stability are significantly needed for elevating MOFs to the applied level.

Herein, we report a novel microporous Zn-based MOF, $[Zn_9(OH)_2\mathbf{L}_6](H_3O)_2(H_2O)_6$ (**1**), where $H_3\mathbf{L}$ = 1,3,5-tri(3-hydroxyl-4-carboxyl)phenylbenzene, synthesized by reaction of $H_3\mathbf{L}$ with zinc nitrate and triethylene diamine in water under hydrothermal reaction condition. As a matter of fact, the material synthesized in water could be expected to possess good water stability and high potential application in humid industrial environment, which has also been verified in this work. In order to investigate its performance for CO_2 removal from syngas which is primarily composed of CO and H_2 in most cases, combination of Monte Carlo (MC) and Ideal Adsorbed Solution Theory (IAST) method, and breakthrough experiment were applied to study the selectivity of CO_2 from syngas/CO_2 mixture. To our knowledge, it is the first report about the CO_2 capture for binary syngas purification using MOFs.

X-Ray crystallographic analysis indicates that **1** crystallizes in a

[a] *State Key Laboratory of Heavy Oil Processing, China University of Petroleum, Beijing 102249, China. E-mail: rzhong@cup.edu.cn*
[b] *College of Engineering, Peking University, Beijing 100871, China. E-mail: rzou@pku.edu.cn*

† Electronic supplementary information (ESI) available: synthesis and characterization of ligand (Scheme S1, Fig. S1-S3), material characterization, gas sorption measurements, breakthrough measurements (Fig. S4), Structure Data (Table S1 and S2), Crystal structure (Fig. S5), FT-IR spectra (Fig. S6), TGA curves (Fig. S7), PXRD data (Fig. S8), Nitrogen adsorption isotherms (Fig. S9), Molecules distribution upon adsorption (Fig. S10), isosteric heat of CO_2 (Fig. S11-S12), and breakthrough curves (Fig. S13). CCDC 1062611. For ESI and crystallographic data in CIF or other electronic format see DOI:10.1039/x0xx00000x

Cubic $P4_132$ space group, consisting of anionic $[Zn_9(OH)_2L_6]^{2-}$ framework and protonated water. The host framework is composed of two crystallographic independent Zn(II) coordinated to **L** ligand and hydroxyl ion. Zn(1) atom adopts tetrahedral coordination mode to one hydroxyl ion and three carboxyl oxygen from separate **L** ligand, in which the bond length of $Zn\text{-}O_{(OH)}$ bond (2.024(3) Å) is longer than that of $Zn\text{-}O_{(COO)}$ (1.940-1.964 Å), indicating much stronger coordination interactions of Zn(II) ion to carboxyl group in this tetrahedron. Zn(2) atom is located in the crystallographic 2-fold axis along with *c* direction with a half occupancy in an asymmetric unit, and coordinates to six carboxyl oxygen atoms in a typical octahedral configuration. The $Zn\text{-}O_{(COO)}$ bonds fall into the range of 2.047 to 2.094 Å, which show slightly weaker coordination bonding interactions than those in tetrahedral configuration. The two crystallographic independent zinc atoms self-assemble into a linear trinuclear Zn_3 molecular building block (MBB) with Zn-Zn separation of 3.562(2) Å. This MBB are bounded together by six carboxyl group in μ_2 fashion from separate **L** ligands (Fig. 1a), which is a typical MBBs in many Zn-based MOFs.[16] The **L** ligand adopts a uniform μ_2 coordination mode to bridge six Zn(II) ions, and these hydroxyl groups do not participate in coordination. Interestingly, three adjacent Zn_3 MBBs are further symmetrically linked together by a μ_3 hydroxyl (-OH) ions to result in three dimensional $[Zn_9(COO)_{18}(OH)_2]^{2-}$ anion network (Fig. 1d,e), in which hydroxyl oxygen atom is located in a crystallographic 3-fold axis along with *b* direction. As shown in Fig. 1e, **1** assembles into a porous trigonal-biyramid-like polyhedron by six intertwined **L** ligands linked by metal clusters with pore diameter of around 1 nm, in which the pores are inconsecutive and separated by ligands (Fig. S5, Supporting Information). These trigonal biyramids are interweaved together to form a 3D network (Fig. 1f).

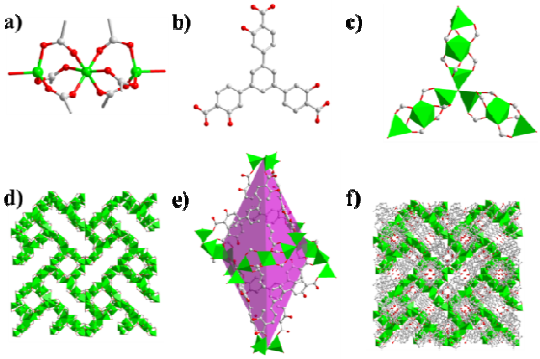

Figure 1 View of crystal structure of **1**: (a) coordination environment of the symmetric trinuclear MBB; (b) L ligands; (c) $Zn_9(COO)_{18}(OH)$ cluster bridged by a μ_3 hydroxyl (-OH) ion; (d) 3D network constructed by $Zn_9(COO)_{18}(OH)$ clusters (organic linkers are omitted for the clarification); (e) porous trigonal-biyramid-like polyhedron (pink) by six intertwined **L** ligands and metal clusters; and (f) 3D network. All hydrogen atoms are omitted for the clarification. Green: Zn, Gray: C, Red: O.

To better understand such a complicated structure, the topology of the anion framework of **1** was studied by using Topos 4.0 software. [17] The network topology is based on 8-connected Zn_3 MBBs and two types of 3-connected nodes from hydroxyl ion and **L** ligand. The structure has a (3,8)-connected (3,8-c) net with stoichiometry $(3\text{-c})_8(8\text{-c})_3$ (Fig. 2). Therefore, **1** self-assembles into a 3D net with the point symbol of $\{4^3;6^9;8^4;10^{12}\}_3\{4^3\}6\{6^3\}_2$. To the best of our knowledge, this is a new (3,8)-connected topology based on the search from RCSR database. (http://rcsr.net/nets)

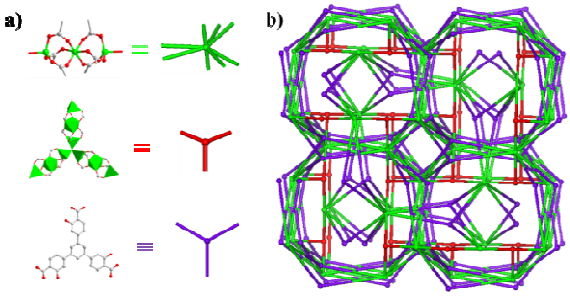

Figure 2 Topological graph of the anion framework of **1**.

Thermogravimetric analysis (TGA) was carried out on crystalline **1** and the TGA curve shows a significant decline before 100 ˚C, indicating the loss of water molecule that occupies the vacancies in the lattice (Fig. S7, Supporting Information). After a subsequent platform up to 270 ˚C, the framework began to collapse according to the sharp decline of the TGA curve.

Furthermore, the framework stability of **1** was studied and characterized by powder X-ray diffraction (PXRD). As shown in the PXRD patterns (Fig. S8, Supporting Information), the peak position of **1** before and after activated at 100 ˚C for 5 hrs are in good agreement with that of the simulated pattern, indicating that **1** retains its framework integrity after the removal of the guest molecules. When the activated sample was soaked in water for 7 days, and even distilled in boiling water for 12 hours, the original crystalline phase of **1** still remained, indicating that **1** exhibits both thermodynamic and kinetic stability in the presence of water.[12, 18] One reason resulting in its good water stability probably is the six-coordinated zinc atom in the center of the trinuclear MBB that is relative robust and render it unfavourable for an irreversible hydrolysis reaction to occur. Moreover, it is worthwhile to note that the four-coordinated zinc atom is usually an unstable coordination mode and is easy to break down through the competitive coordination of water. However in the four-coordinated zinc unit of **1**, besides the coordination to three oxygen atoms from -COO groups in μ_2 mode, there is a μ_3 hydroxyl (-OH) anion coordinated to zinc atom through strong coordination bond which are more competitive than the oxygen atom of water. It is also worth noting that, the p*K*a of the coordination atom on the ligand can be used as a first-order approximation of the metal-ligand bond strength, based on the Lewis acid-base coordination chemistry within MOFs. It was first noted by Long et al. and used as a strategy in the synthesis of a series of highly stable Co-, Zn-, Ni-, and Cu-based MOFs containing the pyrazolate ligand (p*K*a 19.8).[19] While in **1**, the p*K*a of the coordinated oxygen atom of -COO group on the ligand is only 2.02, less than that of the oxygen atom of -COO group on the ligand of MOF-177 (3.46), according to the p*K*a calculation using Advanced Chemistry Development, Inc. (ACD/Labs) software V6.0.[20]. Therefore, the water stability of **1** may be mainly due to the stable coordination modes of zinc atoms in the MBB.

The solvent-accessible volume in **1** is 5122.7 Å^3 that constitutes as high as 29.1% volume per unit cell calculated by PLATON routine,[20b] indicating its porous nature. The permanent porosity of **1** was confirmed by the N_2 adsorption with the largest uptake amount of 156.0 cm^3g^{-1}. The N_2 sorption isotherm of activated **1** exhibits type-I sorption behaviour (Fig. S9) according to the IUPAC classification.[21] Brunauer-Emmett-Teller (BET) surface area of **1** is 439.2 m^2g^{-1}. Furthermore, the adsorption behaviour of **1** for pure CO_2, CO and H_2 was investigated by both MC simulation and gas sorption measurement. CO_2 adsorptive field was calculated by Mont Carlo method and the details have been described in supporting information.[22] For clarification, only Zn-O clusters were shown in Fig 3a. CO_2 were distributed regularly in three regions. First, CO_2 molecules occur around O-H$_{(ZnO)}$ group and H_3O^+ in which H atoms present positive charge and induce quadrupole moment of CO_2. Strong interaction between positive H and CO_2 results in a high uptake of CO_2. Second, CO_2 occur around O-H groups in the **L** ligand which have the same effect on CO_2. Electronic pair of sp2 hybrid O and combined H have special effect on CO_2. Third, CO_2 occur around the space encircled by the ligands which produce a strong potential trap for CO_2 molecules. Comparing with CO_2, CO distributes mainly in the space encircled by the ligands (Fig. S10), demonstrating a different adsorptive mechanism. CO with poor quadrupole moment does not have special effect on the charged H atom. Moreover, the polarizability of CO is less than CO_2 because of strong C-O sigma bond and feedback π bond. Both reasons result in less uptake of CO than that of CO_2. Due to the weak intermolecular force, H_2 scatter in the pore of the **1** without obvious feature. The adsorption amount of CO_2 reaches 51.0 $cm^3\ g^{-1}$ at 273 K and 1 atm, which is much higher than those of CO (3.8 $cm^3\ g^{-1}$) and H_2 (0.5 $cm^3\ g^{-1}$) under the same conditions. It should be noted that the simulated uptakes of CO_2 and CO by MC method in **1** are slightly higher than those of experimental results, which are probably attributed to either part loss of active sites of **1** like protonized water molecules during activation or crystal defects (Fig. 3b). Isosteric Heat of CO_2 calculated by MC simulation is *ca.* 27 KJ/mol, which is agreed with the experimental result (Fig S11-S12). OH group and protonated water contribute a better affinity for CO_2 molecules, compared with CO and H_2 molecules, considering the polarizability (2.63×10^{-40} $J^{-1}C^2m^2$) and the quadrupole moment (-14.3×10^{-40} Cm^2) of CO_2 is much higher than those of CO (1.98×10^{-40} $J^{-1}C^2m^2$, -6.7×10^{-40} Cm^2) and H_2(0.819×10^{-40} $J^{-1}C^2m^2$, 2.12×10^{-40} Cm^2). [23]

The significant difference of uptake amounts makes **1** great promise for the application of CO_2 capture from syngas. The adsorption selectivities of CO_2 over CO at 273 K were calculated by MC simulation and the IAST method. The detailed has been described in supporting information. The volumetric ratio of the gas mixtures for calculation is CO_2: CO: H_2= 1: 1: 1. The selectivities of CO_2/CO and CO_2/H_2 in **1** calculated by IAST method are 27.5 and 858.3 under 1atm and 273 K, which fit well with the calculated results of 36.1 and 865.8 by MC simulation, respectively.

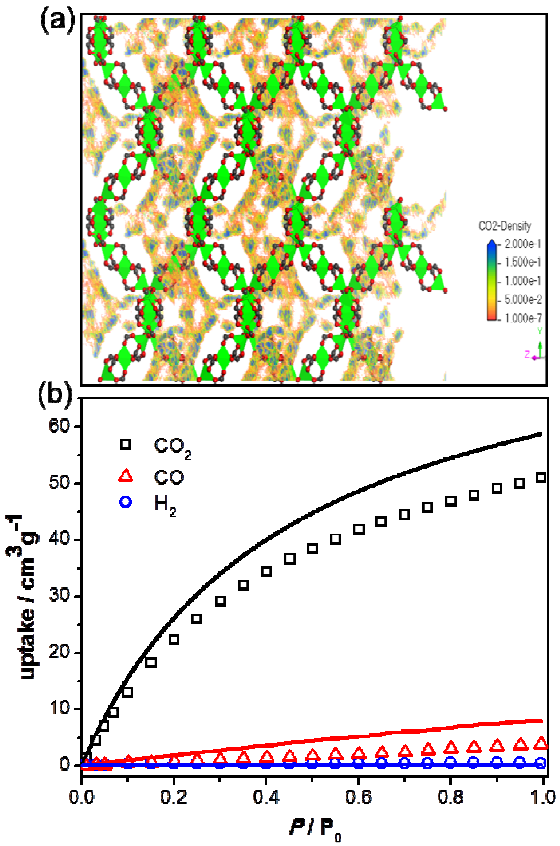

Fig. 3 (a) CO_2 density distribution at 278K under 1 atm, (b) comparison of experimental (symbols) and simulation (lines) sorption isotherms for CO_2 (black), CO (red) and H_2 (blue) at 273K.

To better evaluate the potential of **1** in the separation of CO_2 from syngas/CO_2 mixture in dynamic condition, vapour-phase breakthrough experiments were carried out for the ternary gas mixture composed of 35.04 v% H_2, 19.96 v% CO_2, 10.02 v% CO balanced with Helium. All of the breakthrough curves were recorded by a home-made instrument illustrated in Fig. S4 (Supporting Information). Fig. 4 shows the breakthrough curves obtained at 273 K and a total mixture gas pressure of 0.1MPa. The experimental details can be seen in the Supporting Information. A clear difference in breakthrough time between CO_2 and syngas was observed. After an initial period during which all three components were fully absorbed, H_2 was first eluted, followed by CO. The concentration of syngas at the outlet exceeds the inlet concentration because the absorbed CO_2 molecules displace part of the adsorbed syngas molecules. Finally CO_2 started to be eluted and the concentration of all components gradually reached the feed concentration level, indicating the absorption bed was saturated. As expected, for the CO_2/syngas mixture, CO_2 is the more adsorbed component when it is present. CO_2 might have the strongest interaction with electric field of framework of **1** due to its high polarizability and great quadrupole moment. The following order of the adsorption capability of **1** can be derived from Fig. 4: CO_2 > CO > H_2, which is in fair agreement with the order of their pure component equilibrium. The same phenomenon was also observed in the breakthrough curves of the

gas mixture with the same volumetric ratio at 1MPa (Fig. S13, Supporting Information).

The separation efficiency for the ternary mixture can be simplified and compared in terms of sorption selectivity, S, defined as $S = (n_i/n_j)/(C_i/C_j)$, where component *i* is the more adsorbed, and n and *C* represent the concentration of components and amount adsorbed respectively. The calculated $S_{CO2/H2}$ is 49.2 and $S_{CO2/CO}$ is 5.1, indicating that **1** exhibits a higher selectivity for CO_2, which is a promising candidate for CO_2/syngas separation.

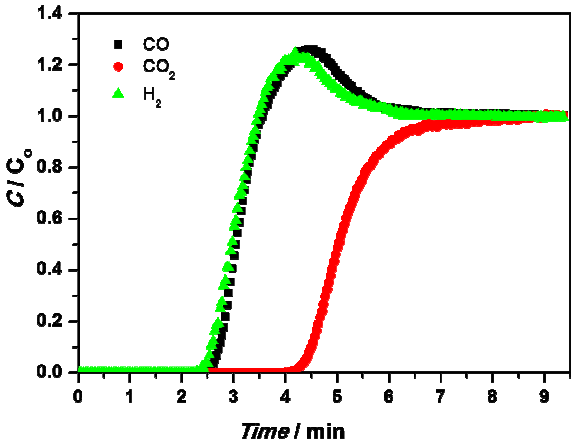

Fig. 4 Breakthrough curves of **1** at 273 K and a total mixture gas pressure of 0.1MPa.

Conclusions

In summary, we have succeeded in preparing a water-stable Zn-based metal-organic framework with (3,8)-connected topology and applied for CO_2 removal from binary syngas for the first time. The water stability of **1** may be mainly due to the stable coordination modes of zinc atoms in the MBB. The real gas separation for CO_2 from syngas carried out by the breakthrough experiments has verified the potential application for syngas purification which has been primarily suggested by simulation and IAST prediction. Moreover, the high water stability of the material may pave the way for practical usage of syngas purification. Future research will focus on design and synthesis of water-stable frameworks with higher surface areas and greater capacities for CO_2 storage.

The authors are grateful to the support of the NSFC (No. 21203249 and 21406004) and the Science Foundation of China University of Petroleum, Beijing (No. 01JB0229).

Notes and references

† Synthesis and activation of **1**: $Zn(NO_3)_2 \cdot 6H_2O$ (0.045g, 0.15mmol), H_3**L** (0.024g, 0.05mmol), triethylene diamine (0.033g, 0.15mmol) and 15 mL H_2O were added into a 20 mL scintillation vial. The mixture was sonicated at room temperature until clear and then transferred to a 25 mL Teflon-lined steel autoclave. The autoclave was sealed, gradually heated to 140 ºC within 12 h and then kept at this temperature for 72 h. After slowly cooling down to room temperature within 48 h, the colorless column crystals were obtained. The crystals were filtered out and washed with distilled water for 3 times. The solvent within the pores of the resulting solid was removed under dynamic vacuum at 100 ºC for 5 h. Yield: 31% (based on H3L). IR (cm–1): 3423br, 1628m, 1581s, 1508m, 1414s, 1363m, 1257m, 1196m, 1163w, 958w, 831w,785w. w=weak, s=strong, m=medium, br=broad. Anal. Calcd for C162H110O64Zn9: C, 53.03; H, 3.02 %. Found: C, 53.26; H, 3.58 %.

‡ The crystal data were collected on a Bruker APEXII CCD Detector single-crystal X-ray diffractometer at room temperature with Mo-Kα radiation (λ = 0.71073 Å). The structures were solved by direct methods using the SHELXS program of the SHELXTL package and refined by full-matrix least-squares methods with SHELXL[24]. Zn atoms in each complex were located from the E-maps and other non-hydrogen atoms were located in successive difference Fourier syntheses, which were refined with anisotropic thermal parameters on F_2. The hydrogen atoms of the ligands were generated theoretically onto the specific atoms and refined isotropically with fixed thermal factors. Solvent molecules in the structure were randomly dispersed, and thus their positions were impossible to refine using conventional discrete-atom models. Crystal data for **1**: cubic, space group *P*4(1)32 with a = 26.01190(10) Å, b = 26.01190(10) Å, c = 26.01190(10) Å, β = 90.00º, V = 17600.14(12) Å^3, Z = 4, ρ_{calcd} = 1.344 g/cm^3. R_1 = 0.0760, R_{w2} = 0.2333, and GOF = 1.057. CCDC-1062611 contains the supplementary crystallographic data for this paper. It should be noted that there are some free water molecules in the cage of **1** without being refined due to their poor diffraction. These data can be obtained free of charge via www.ccdc.cam.ac.uk/conts/retrieving.html (or from the Cambridge Crystallographic Data Centre, 12 Union Road, Cambridge CB21EZ, UK; fax: (+44) 1223-336-033; or deposit@ccdc.cam.ac.uk).

Electronic Supplementary Information (ESI) available: [details of any supplementary information available should be included here]. See DOI:10.1039/c000000x/

1 National Research Council (NRC), *Advancing the Science of Climate Changes*, The National Academies Press, Washington, DC, USA, 2010.
2 J. R. Hufton, S. Mayorga and S. Sircar, *AIChE J.*, 1999, **45**, 248−256.
3 C. T. Chou and C. Y. Chen, *Sep. Purif. Technol.*, 2004, **39**, 51–65.
4 M. Eddaoudi, D. B. Moler, H. Li, B. Chen, T. M. Reineke, M. O'Keeffe and O. M. Yaghi, *Acc. Chem. Res.,* 2001, **34**, 319−330.
5 Z. Zhang, Z. Yao, S. Xiang and B. Chen, *Energy Environ. Sci.*, 2014, **7**, 2868–2899.
6 (*a*) V. Chandrasekhar, C. Mohapatra, R. Banerjee and A. Mallick, *Inorg. Chem.*, 2013, **52**, 3579−3581; (*b*)D. Nagaraju, D. G. Bhagat, R. Banerjee and U. K. Kharul, *J. Mater. Chem. A.*, 2013, **1**, 8828−8835; (*c*)J. R. Li, Y. Ma, M. C. McCarthy, J. Sculley, J. Yu, H. K. Jeong, P. B. Balbuena and H. C. Zhou, *Coord. Chem. Rev.,* 2011, **255**, 1791−1823; (*d*) Y. Liu, D. Liu, Q. Yang, C. Zhong and J. Mi, *Ind. Eng. Chem. Res.,* 2010, **49**,2902–2906; (*e*) Q. Yang and C. Zhong, *J. Phys. Chem. B,* 2006, **110**, 17776–17783; (*f*) J. Jiang, *AIChE J.,* 2009, **55**, 2422–2432; (*g*) R. Babarao, M. Eddauodi and J.W. Jiang, *Langmuir,* 2010, **26**, 11196–11203; (*g*) R. Babarao and J.W. Jiang, *Ind. Eng. Chem. Res.,* 2011, **50**, 62–68; (*h*) D. Wu, Q. Xu, D. Liu and C. Zhong, *J. Phys. Chem. C,* 2010, **113**, 16611–16617; (*i*) Y. Chen and J. Jiang, *ChemSusChem,* 2010, **3**, 982–988; (*j*) Z.R. Herm, J.A. Swisher, B. Smit, R. Krishna and J.R. Long, *J. Am. Chem. Soc.,* 2011, **133**, 5664–5667.
7 (*a*)M. Chen, H. Zhao, C. Liu, X. Wang, H. Shi and M. Du, *Chem. Commun.*, 2015, **51**, 6014–6017; (*b*) D. M. Chen, X.P. Zhang, W. Shi and P. Cheng, *Inorg. Chem.,* 2015, **54**, 5512−5518; (*c*) M. Du, C. Li, M. Chen, Z. Ge, X. Wang, L. Wang and C. Liu, *J. Am. Chem. Soc.*, 2014, **136**, 10906–10909.
8 (*a*) L. Hamon, P. L. Llewellyn, T. Devic, A. Ghoufi, G. Clet, V.Guillerm, G. D. Pirngruber, G. Maurin, C. Serre, G. Driver,

W.van Beek, E. Jolimaitre, A. Vimont, M. Daturi and G. Férey, *J.Am. Chem. Soc.* 2009, **131**, 17490–17499; (*b*) B. Wang, A. P. Côté, H. Furukawa, M. O'Keeffe and O. M. Yaghi, *Nature*, 2008, **453**, 207–211.

9 (*a*) Ö. Yazaydin, R. Q. Snurr, T. H. Park, K. Koh, J. Liu, M. D. LeVan, A. I. Benin, P. Jakubczak, M. Lanuza, D. B. Galloway, J. J. Low and R. R. Willis, *J. Am. Chem. Soc.*, 2009, **131**, 18198–18199; (*b*) J. A. Mason, K. Sumida, Z. R. Herm, R. Krishna and J. R. Long, *Energy Environ.Sci.,* 2011, **4**, 3030–3040; (*c*) Z. Liang, M. Marshall and A. L. Chaffee, *Energy Fuels,* 2009, **23**, 2785–2789; (*d*) S. R. Caskey, A. G. Wong-Foy and A. J. Matzger, *J. Am. Chem. Soc. ,* 2008, **130**, 10870–10871; (*e*) J. S. Lee, J. H. Kim, J. T. Kim, J. K. Suh, J. M. Lee and C. H. Lee, *J. Chem. Eng. Data.,* 2002, **47**, 1237–1242; (*f*) Y. Wang and M. D. LeVan, *J. Chem. Eng. Data.,* 2009, **54**, 2839–2844; (*g*) T. H. Bae, M. R. Hudson, J. A.Mason, W. L. Queen, J. J. Dutton, K. Sumida, K. J. Micklash, S. S. Kaye, C. M. Brown and J. R. Long, *Energy Environ. Sci.,* 2013, **6**, 128–138; (*h*) D. Britt, H. Furukawa, B. Wang, T. G. Glover, and O.M. Yaghi, *Proc. Natl. Acad. Sci. U.S.A.*, 2009, **106**, 20637–20640; (*i*) P. D. C. Dietzel, V. Besikiotis and R. J. Blom, *Mater. Chem.,* 2009, **19**, 7362–7370; (*j*) H. Wu, J. M. Simmons, G. Srinivas, W. Zhou and T. J. Yildirim, *Phys. Chem. Lett.,* 2010, **1**, 1946–1951; (*k*) L. Valenzano, B. Civalleri, S. Chavan, G. T. Palomino, C. O. Arean and S. J. Bordiga, *J. Phys. Chem. C,* 2010, **114**, 11185–11191; (*l*) Z. Bao, L. Yu, Q. Ren, X. Lu and S. J. Deng, *Colloid Interface Sci.,* 2011, **353**, 549–556.

10 K. Sumida, D. L. Rogow, J. A. Mason, T. M. McDonald, E. D. Bloch, Z. R. Herm, T. H. Bae and J. R. Long, *Chem. Rev.*, 2012, **112**, 724–781.

11 R. Bararao and J. Jiang, *J. Am. Chem. Soc.*, 2009, **131**, 11417–11425.

12 C. B. Nicholas, J. Himanshu and S. W. Krista, *Chem. Rev.,* 2014, **114**, 10575−10612.

13 (*a*) O. M. Yaghi, H. Li, M. Eddaoudi and M. O'Keeffe, *Nature,* 1999, **402**, 276–279; (*b*) M. Eddaoudi, J. Kim, N. Rosi, D. Vodak, J. Wachter, M. O'Keeffe and O. M. Yaghi, *Science*, 2002, **295**, 469–472.

14 (*a*) L. Bellarosa, J. M. Castillo, T. Vlugt, S. Calero and N. López, *Chem. Eur. J.*, 2012, **18**, 12260–12266; (*b*) M. D.Toni, R. Jonchiere, P. Pullumbi, F. X. Coudert and A. H. Fuchs, *ChemPhysChem*, 2012, **13**, 3497–3503; (*c*) M. Sabo, A. Henschel, H. Frçde, E. Klemm and S. Kaskel, *J. Mater. Chem.*, 2007, **17**, 3827–3832; (*d*) J. A. Greathouse and M. D. Allendorf, *J. Am. Chem. Soc.,* 2006, **128**, 10678–10679.

15 (*a*) J. Liu, A. I. Benin, A. M. B. Furtado, P. Jakubczak, R. R. Willis and M. D. LeVan, *Langmuir,* 2011, **27**, 11451–11456; (*b*) A. C. Kizzie, A. G. Wong-Foy and A. J. Matzger, *Langmuir,* 2011, **27**, 6368–6373.

16 R. Zou, R. Zhong, S. Han, H. Xu, A. Burrell, N. Henson, J. L. Cape, D. D. Hickmott, T. V. Timofeeva and T. E. Larson, *J. Am. Chem. Soc.*, 2010, **132** ,17996–17999.

17 (*a*) M. O'Keeffe, M. A. Peskov, S. J. Ramsden and Omar M. Yaghi, *Acc. Chem. Res.*, 2008, **41**, 1782–1789; (*b*) S. R. Batten, N. R. Champness, X. Chen, J. Garcia-Martinez, S. Kitagawa, L. Öhrström, M. O'Keeffe, M. P. Suh and J. Reedijk, *Pure Appl. Chem.*, 2013, **85**, 1715–1724.

18 (*a*) M. Du, M. Chen, X. Yang, J. Wen, X. Wang, S. Fang and C. Liu, *J. Mater. Chem. A*, 2014, **2**, 9828–9834; (*b*) T. Li, D. Chen, J. E. Sullivan, M. T. Kozlowski, J. K. Johnson and N. L. Rosi, *Chem. Sci.*, 2013, **4**, 1746–1755; (*c*) D. Feng, W. Chung, Z. Wei, Z. Gu, H. Jiang, Y. Chen, D. J. Darensbourg, H. Zhou, *J. Am. Chem. Soc.*, 2013, **135**, 17105–17110; (*d*) H. Furukawa, F. Gandara, Y. Zhang, J. Jiang, W. L. Queen, M. R. Hudson, O. M. Yaghi, *J. Am. Chem. Soc.*, 2014, **136**, 4369–4381; (*e*) F. Jeremias, A.Khutia, S. K. Henninger, C. Janiak, *J. Mater. Chem.*, 2012, **22**, 10148–10151; (*f*) D. Cunha, M. B.Yahia, S. Hall, S. R.Miller,; H. Chevreau, E. Elkaim, G. Maurin, P. Horcajada, C. Serre, *Chem. Mater.*, 2013, **25**, 2767–2776.

19 (*a*) H. J. Choi, M. Dinca, A. Dailly, J. R. Long, *Energy Environ. Sci.*, 2010, **3**, 117; (*b*) V. Colombo, S. Galli, H. J. Choi, G. D. Han, A. Maspero, G. Palmisano, N. Masciocchi, J. R. Long, *Chem. Sci.*, 2011, **2**, 1311–1319.

20 (*a*) ACD/Structure Elucidator, version 6.0, Advanced Chemistry Development, Inc., Toronto, ON, Canada, www.acdlabs.com, 2014; (*b*) A. L. Spek, *PLATON, A Multipurpose Crystallographic Tool*, Utrecht University, Utrecht, The Netherlands, 2001.

21 K. Sing, D. Everett, R. Haul, L. Moscou, R. Pierotti, J. Rouquerol and T. Siemieniewska, *Pure Appl. Chem.*, 1985, **57**, 603–619.

22 (*a*) B. Supronowicz, A. Mavrandonakis and T. Heine, *J. Phys. Chem. C*, 2013, **117**, 14570–14578; (*b*) L. Hamon, H. Leclerc, A. Ghoufi, L. Oliviero, A. Travert, J. C. Lavalley, T. Devic, C. Serre, G. Férey, G. D. Weireld, A. Vimont and G. Maurin, *J. Phys. Chem. C*, 2011, **115**, 2047–2056; (*c*) H. Guo, F. Shi, Z. Ma, X. Liu, *J. Phys. Chem. C*, 2010, **114**, 12158–12165.

23 C. J. F. Böttcher and P. Bordewijk, *Theory of Electric Polarization*, Elsevier, Amsterdam, 1978.

24 G. M. Sheldrick, *SHELXTL NT*, *Program for Solution and Refinement of Crystal Structures, version 5.1*, University of Göttingen, Germany, 1997.

Graphical Abstract

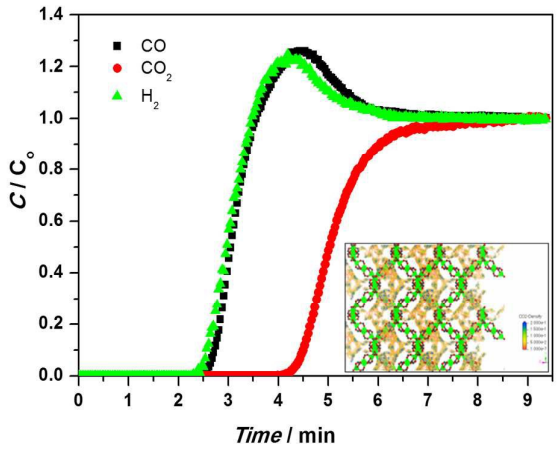

The experimental and theoretical investigation of a new water-stable Zn-based metal-organic framework for CO_2 removal from syngas (binary gas mixture of CO and H_2) is presented.